Chemical Engineering & Processing: Process Intensification 224 (2026) 110796

Contents lists available at ScienceDirect

Chemical Engineering and Processing - Process Intensification

journal homepage: www.elsevier.com/locate/cep

Process intensification of multi-stage heat pump assisted distillation with liquid injection

Chengtian Cui [a,b,*], Anton A. Kiss [b,**]

[a] Process and Systems Engineering Laboratory, Åbo Akademi University, Henrikinkatu 2, 20500 Turku, Finland
[b] Department of Chemical Engineering, Delft University of Technology, Van der Maasweg 9, 2629 HZ, Delft, the Netherlands

ARTICLE INFO

Keywords:
Process intensification
Electrification
Heat pump assisted distillation
Liquid injection

ABSTRACT

Multi-stage mechanical vapor recompression (MVR) is a promising route to electrify and intensify distillation for wide-boiling separations, yet its deployment is often constrained by the requirements for effective inter-stage cooling and utilization of the associated sensible heat. This work proposes and evaluates liquid injection as a compact intensification alternative to conventional exchanger-based intercooling in a two-stage MVR system. Unlike prior work on the discretely heat integrated distillation column (D-HIDiC), this study introduces liquid injection directly into MVR systems, eliminating intercooler hardware while maintaining energy performance. Four configurations are examined: a two-stage MVR without intercooling (**MVR #1**), an intercooled MVR with internal heat recovery to an additional bottom reboiler (**MVR #2**), a liquid injection MVR without an intercooler (**MVR #3**), and a liquid injection MVR combined with pre-compressor splitting (**MVR #4**) to mitigate the increased second-stage compressor load caused by injection. Compared with conventional distillation (CDiC, 10,073 kW reboiler duty), all MVR cases reduce the final energy input to 1759–1850 kW (81.6–82.5% savings) with COP values of 5.445–5.727; **MVR #4** achieves the lowest compressor power (1759 kW) and the highest COP (5.727). On a primary-energy basis (36.6% electricity conversion efficiency), the MVR schemes deliver 49.8–52.3% savings versus CDiC. Overall, liquid injection enables equipment simplification with competitive efficiency, while pre-compressor splitting provides a practical tuning degree of freedom to recover or improve performance without sacrificing compactness.

1. Introduction

Distillation is the most widely used separation technology in the process industries, but it is also the most energy-intensive. It accounts for approximately 95% of the energy consumption in liquid-phase separations and around 2.5% of the total energy use in the United States [1]. Conventional distillation columns (CDiCs) typically rely on fossil fuel combustion to supply thermal energy. In the context of increasing global efforts toward carbon neutrality and energy transition, improving the energy efficiency and sustainability of distillation processes has become a critical priority [2].

Electrifying the heat supply using renewable electricity via heat pumps offers a promising pathway to intensify distillation processes [3–8]. Heat pump assisted distillation (HPAD) leverages external power to upgrade waste heat and to provide the reboiler duty at a higher temperature level, thereby reducing or even eliminating the need for fossil-based steam [9]. Among various HPAD options, mechanically driven systems are particularly attractive for process electrification. Mechanical vapor recompression (MVR) upgrades the enthalpy of overhead vapor by direct compression. Vapor compression (VC) using external working fluids allows more flexibility in thermal matching, while heat integrated distillation column (HIDiC) with internal heat recovery can maximize energy efficiency [10].

Most HPAD studies have focused on single-stage MVR, which is generally economical only for mixtures with small boiling point differences (ΔT_b) [10]. For a given temperature driving force (ΔT_{df}), the required compression duty is directly proportional to the temperature lift ($\Delta T_{lift} = \Delta T_b + \Delta T_{df}$) that needs to be overcome, as can be understood from the ideal adiabatic (isentropic) compression of an ideal gas [11]:

* Corresponding author at: Process and Systems Engineering Laboratory, Åbo Akademi University, Henrikinkatu 2, 20500 Turku, Finland.
** Corresponding author.
E-mail addresses: Chengtian.Cui@abo.fi (C. Cui), A.A.Kiss@tudelft.nl (A.A. Kiss).

https://doi.org/10.1016/j.cep.2026.110796
Received 30 December 2025; Received in revised form 11 February 2026; Accepted 2 April 2026
Available online 3 April 2026

$$W = F\left(\frac{\gamma}{\gamma-1}\right)RT_{in}\left[\left(\frac{P_{out}}{P_{in}}\right)^{(\gamma-1)/\gamma}-1\right] \quad (1)$$

where W is the compression power $[kW]$, F flow rate $\left[kmol{\cdot}s^{-1}\right]$, R the ideal gas constant 8.314 $J{\cdot}mol^{-1}{\cdot}K^{-1}$, T_{in} inlet temperature $[K]$, P_{in} and P_{out} are inlet and outlet pressures $[Pa]$, and γ heat capacity ratio C_P/C_V (1.4 for ideal gas).

As the ΔT_{lift} increases, the corresponding pressure ratio $\Pi = P_{out}/P_{in}$ increases, and the compression work rises accordingly ($W \propto P_{out}/P_{in} \propto \Delta T_{lift}$). In practice, the pressure ratio for single-stage compression typically lies in the range of 2.5 to 4.0 [12]. Beyond this range, multi-stage compression is needed to extend the applicability of MVR to systems that require larger temperature lifts.

Applications of multi-stage MVR in distillation have been reported in the literature [13–15]. However, many of these implementations do not include inter-stage cooling, which leads to elevated compression power in the downstream stages. This follows directly from Eq. (1), since the compression work is proportional to the inlet temperature ($W \propto T_{in}$). Inter-stage cooling therefore becomes a critical design consideration in multi-stage MVR systems. Traditionally, this cooling is achieved using external heat exchangers that reject heat to ambient or to process utility streams [16]. The sensible heat removed in this way still carries waste heat at a moderate temperature. If recovered properly, this heat can be reintegrated into the distillation system — for example, as duty for the main reboiler [17] or for side reboilers via pump around loops [18]. This motivates the development of novel designs that utilize intercooling heat internally rather than dissipating it, which is the focus of this study.

To enable more effective utilization of intercooling heat, our recent work [18] introduced the concept of liquid injection in a discretely HIDiC (D-HIDiC). The basic concept is that a portion of the high-pressure column bottoms liquid is injected between compressor stages. Compared to a pump around loop, liquid injection offers a more compact solution that eliminates the need for additional heat exchangers. In addition, the integration of liquid injection also shows robust dynamic controllability [19].

Liquid injection between compression stages is not a new concept. In refrigeration, building HVAC (heating, ventilation, and air conditioning), and high-temperature heat pump applications, intermediate injection (most papers called this as “vapor injection” [20,21]) has long been used as an effective means of inter-stage cooling and discharge temperature control, and is often discussed together with economizer/flash-tank schemes and intermediate pressure optimization to improve COP (coefficient of performance) and widen the feasible operating window [22]. Recent studies continue to analyze such intercooling/injection effects for two-stage vapor compression heat pumps under low-temperature and high lift conditions, confirming the potential of intermediate injection to moderate discharge temperature and improve efficiency [23,24]. Importantly, most existing works in this area focus on closed-loop cycles. In contrast, a distillation-integrated MVR heat pump operates effectively as an open-loop system. This might explain why liquid injection intercooling is rarely reported in column-integrated multi-stage MVR configurations.

Against this background, the novelty of the present work lies not in the generic concept of injection-based intercooling itself, but in its translation to an open-loop, distillation-integrated multi-stage MVR configuration and its assessment on a consistent basis. To the best of our knowledge, this study is among the first to (i) apply liquid injection directly within a multi-stage MVR loop integrated with a distillation column for wide-boiling separations, (ii) introduce pre-compressor splitting as an additional intensification lever that provides a tunable degree of freedom to recover or improve COP while retaining a compact compression train, and (iii) benchmark MVR schemes (with and without injection/splitting) against both CDiC and D-HIDiC under identical column specifications, separation duties, and thermodynamic assumptions. These elements collectively define the effective contribution of the article: demonstrating that a two-stage MVR with injection can eliminate an exchanger-based intercooler while maintaining competitive energy performance, and that pre-compressor splitting can mitigate the injection-induced compressor duty penalty in a way that is directly relevant to electrified distillation.

2. Problem statement

While MVR is widely recognized for electrifying distillation, existing studies largely focus on single-stage compression, which is suitable only for close-boiling mixtures; for wide-boiling mixtures the required pressure ratio often exceeds the practical range. Multi-stage MVR offers a viable solution to overcome these constraints, but introduces additional challenges, particularly the need for inter-stage cooling and the effective utilization of the associated intercooling heat. This work aims to address these challenges by applying liquid injection as an alternative to exchanger-based intercooling in multi-stage MVR systems. The objectives of this study are as follows:

- Quantify energy savings of multi-stage MVR compared to CDiC and D-HIDiC.
- Assess the impact of liquid injection and pre-compressor splitting on compressor duty and COP.
- Evaluate primary-energy savings of multi-stage MVR relative to CDiC and HIDiC, accounting for the upstream conversion efficiency of electricity.
- Provide thermodynamic insights into the proposed configurations using P–h and T–s representations to interpret operational trajectories and feasibility.
- Discuss the indicative economic implications of the alternative configurations based on the resulting energy duties and equipment sizes.

Although dynamic controllability is a key concern of liquid injection, prior work has established that it does not introduce adverse dynamic interactions [19]. Therefore, dynamic analysis and controllability are not the focus of this steady-state evaluation.

3. Process design

3.1. Processes studied

To enable a direct comparison with the previous work on D-HIDiC, we consider the same case study [18]: separation of a 1000 kmol/h equimolar methanol/water feed at 1 bar and saturated liquid conditions. The required purities of both methanol and water products are 99.99 mol%. The normal boiling points of methanol and water are 64.7 °C and 100 °C, respectively, giving a boiling point difference of $\Delta T_b = 35.3\ ^\circ C$. With an additional temperature driving force of $\Delta T_{df} = 10\ ^\circ C$, the required temperature lift becomes $\Delta T_{lift} = \Delta T_b + \Delta T_{df} = 45.3\ ^\circ C$, which can be characterized as a large temperature lift. All steady-state process simulations are carried out in Aspen Plus V14 using the non-random two-liquid (NRTL) thermodynamic model with built-in parameters.

Four two-stage MVR configurations are investigated in this work (Fig. 1). **MVR #1** (Fig. 1**a**) is a conventional two-stage MVR without inter-stage cooling, as reported in the literature [13–15]. In mixtures such as hydrocarbons with overhanging P–h diagrams, a superheater is needed to prevent partial condensation during compression [25], whereas methanol and water exhibit bell-shaped P–h diagrams and naturally become superheated upon compression; therefore, the superheater is not required and is shown with dashed lines. Since compressing superheated vapor increases power consumption, intercooling is introduced in **MVR #2** (Fig. 1**b**) to recover a portion of the sensible heat generated during the first-stage compression. The recovered heat can be used to supply to either side reboilers or an additional bottom reboiler.

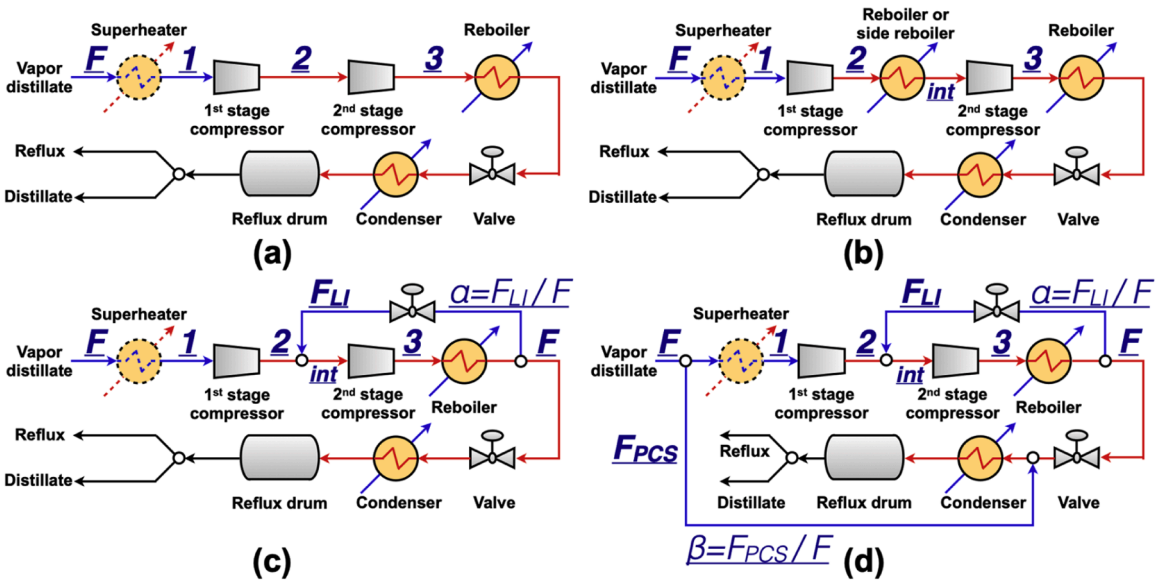

Fig. 1. (a) MVR without intercooling (MVR #1); (b) MVR with intercooling (MVR #2); (c) MVR with liquid injection (MVR #3); (d) MVR with liquid injection and pre-compressor splitting (MVR #4).

However, our previous work [18] shows that the heat supplied to side reboilers does not fully translate into a reduction in main reboiler duty, resulting in an energy penalty. Therefore, whenever temperature driving force allows, the recovered intercooling heat is directed to an additional bottom reboiler. An intensified alternative to external intercooling is liquid injection, implemented in **MVR #3** (Fig. 1**c**). In this configuration, a fraction of the high-pressure condensate (from the recompressed overhead vapor after the main reboiler) is injected between the two compressor stages. Direct-contact cooling eliminates one heat exchanger and provides a more compact design, but it also increases the vapor flow rate entering the second-stage compressor, thereby potentially increasing the second-stage compression duty. To mitigate this drawback, **MVR #4** (Fig. 1**d**) combines liquid injection with pre-compressor splitting. A fraction of the overhead vapor is bypassed before the first-stage compressor and sent directly to the condenser, thereby reducing the vapor load through the compression train and balancing the overall compression duties. The four configurations are simulated under identical column specifications and compression pressure levels, and their steady-state performances are compared in the following sections.

3.2. Key design variables and analytical rationale

This section provides the analytical rationale for selecting the key design variables in the four two-stage MVR configurations. Specifically, the key design variables are:

(i) total pressure ratio $\Pi_{tot} = P_3/P_1$ (or the final discharge pressure P_3);
(ii) inter-stage pressure P_2 (or stage pressure ratio $\Pi_1 = P_2/P_1, \Pi_2 = P_3/P_2$);
(iii) inter-stage cooled/mixed temperature T_{int} (**MVR #2 – #4**);
(iv) liquid injection fraction α (**MVR #3** and **#4**); and
(v) pre-compressor split ratio β (**MVR #4**).

As the objective is to reduce the total compressor power, we use a simplified analytical method based on ideal gas isentropic compression Eq. (1) to illustrate how these key variables affect compression work. This analysis provides physical insight and justifies the variable selection; quantitative values are obtained from rigorous Aspen Plus simulations in Section 4.

For **MVR #1**, we denote (P_1, T_1), $(P_2,\ T_2)$, and $(P_3,\ T_3)$ as the initial, intermediate and final pressures/temperatures, respectively. The total compressor power is:

$$W_{\#1} = F\left(\frac{\gamma}{\gamma-1}\right)RT_1\left[\left(\frac{P_2}{P_1}\right)^{(\gamma-1)/\gamma} - 1\right] + F\left(\frac{\gamma}{\gamma-1}\right)RT_2\left[\left(\frac{P_3}{P_2}\right)^{(\gamma-1)/\gamma} - 1\right] \tag{2}$$

To simplify the analytical comparison and isolate the effect of the key pressure variables, we assume equal stage pressure ratios (the assumption is also used in the following processes):

$$\Pi = \frac{P_2}{P_1} = \frac{P_3}{P_2} \tag{3}$$

Under Eq. (3), Eq (2) becomes:

$$W_{\#1} = F\left(\frac{\gamma}{\gamma-1}\right)R(T_1+T_2)\left[\Pi^{(\gamma-1)/\gamma} - 1\right] \tag{4}$$

Most industrial compression processes are approximately adiabatic; adiabatic compression of an ideal gas along an isentropic path gives:

$$PV^{\gamma} = const \tag{5}$$

Substituting $V = RT/P$ for isentripic compression of an ideal gas gives:

$$\frac{T_2}{T_1} = \left(\frac{P_2}{P_1}\right)^{(\gamma-1)/\gamma} = \Pi^{(\gamma-1)/\gamma} \tag{6}$$

Combining Eqs. (4) and (6) gives:

$$W_{\#1} = F\left(\frac{\gamma}{\gamma-1}\right)RT_1\left[\Pi^{2(\gamma-1)/\gamma} - 1\right] \tag{7}$$

For **MVR #2**, the introduction of an inter-stage cooling step reduces the temperature entering the second-stage compressor. Therefore, the key variable (iii) is the inter-stage temperature T_{int} (i.e. the second-stage inlet temperature). Physically, T_{int} must satisfy two bounds: (1) it should not exceed the first-stage discharge temperature without cooling, and (2) it must remain to be vapor phase to avoid condensation/two-phase flow in the compressor. Accordingly, the feasible range of T_{int} can be expressed as:

$$\max\left(T_{sat}(P_2),\ T_1\right) \le T_{int} \le T_1\Pi^{(\gamma-1)/\gamma} \tag{8}$$

To parameterize the cooling level, we assume $T_{int} = \lambda T_1$, so that:

$$\max\left(T_{sat}(P_2)/T_1,\ 1\right) \le \lambda \le \Pi^{(\gamma-1)/\gamma} \tag{9}$$

Under the equal stage pressure ratio assumption Eq. (3), the total compressor power becomes:

$$W_{\#2} = F\left(\frac{\gamma}{\gamma-1}\right)R(\lambda+1)T_1\left[\Pi^{(\gamma-1)/\gamma}-1\right] \tag{10}$$

It is straightforward to compare the total compressor powers based on Eqs. (7) and (10):

$$\frac{W_{\#1}}{W_{\#2}} = \frac{\Pi^{(\gamma-1)/\gamma}+1}{\lambda+1} \ge 1 \tag{11}$$

Eq. (11) indicates that, for fixed pressure ratios and neglecting additional pressure drop introduced by the intercooling device, inter-stage cooling reduces the total compressor power relative to **MVR #1**.

For **MVR #3**, liquid injection is introduced as a direct-contact inter-stage cooling mechanism. In the analytical treatment, liquid injection can be regarded as a pseudo-intercooler that reduces the inter-stage temperature to a specified value T_{int}. We denote the liquid injection flow rate as F_{LI}, which is used to cool the inter-stage vapor to T_{int}. The key design variable (iv) is defined as the liquid injection fraction $\alpha = F_{LI}/F$ $(\alpha \ge 0)$. Once the target inter-stage temperature is specified (e.g., $T_{int} = \lambda T_1$ as defined in **MVR #2**), the required α can be determined from an energy balance of the mixing step (implemented rigorously in Aspen Plus); here, α is retained as an explicit parameter to illustrate its impact on compressor power. In this case, the total compressor power is:

$$W_{\#3} = F\left(\frac{\gamma}{\gamma-1}\right)RT_1\left[\Pi^{(\gamma-1)/\gamma}-1\right] + F(\alpha+1)\left(\frac{\gamma}{\gamma-1}\right)R\lambda T_1\left[\Pi^{(\gamma-1)/\gamma}-1\right] \tag{12}$$

Or equivalently:

$$W_{\#3} = W_{\#2} + \alpha F\left(\frac{\gamma}{\gamma-1}\right)R\lambda T_1\left[\Pi^{(\gamma-1)/\gamma}-1\right] \tag{13}$$

Eq. (13) highlights the key trade-off of liquid injection: while injection can reduce the inter-stage temperature, it also increases the vapor flow entering the second-stage compression, which directly increases the compressor duty. Therefore, for a fixed target T_{int} and fixed pressure ratios, $W_{\#3} \ge W_{\#2}$, with equality only when $\alpha = 0$. This explains why liquid injection is primarily a hardware-intensification option by eliminating the exchanger-based intercooler rather than an automatic energy advantage, unless additional degrees of freedom are introduced as in **MVR #4**.

Liquid injection increases compressor power primarily because it increases the flow rate entering the second-stage compression. To make the liquid injection concept competitive with exchanger-based inter-stage cooling, **MVR #4** introduces an additional key design variable (v), the pre-compressor split ratio β, defined as $\beta = F_{PCS}/F$ $(0 \le \beta \le 1)$:

$$W_{\#4} = F(1-\beta)\left(\frac{\gamma}{\gamma-1}\right)RT_1\left[\Pi^{(\gamma-1)/\gamma}-1\right] + F(\alpha+1)(1-\beta)\left(\frac{\gamma}{\gamma-1}\right)R\lambda T_1\left[\Pi^{(\gamma-1)/\gamma}-1\right] \tag{14}$$

When $\beta = 0$ (no bypass), Eq. (14) reduces to Eq. (12). When $\beta = 1$, the overhead vapor is routed directly to the condenser without recompression.

Because $W_{\#4}$ depends on multiple coupled variables $(\Pi,\ \lambda,\ \alpha,\ \beta)$, an analytical comparison between **MVR #2** and **MVR #4** is not always straightforward for realistic operating constraints. Therefore, we perform rigorous Aspen Plus simulations to quantify the combined effects and to identify feasible operating ranges of $\alpha$and βunder identical column specifications and pressure levels.

4. Results and discussion

4.1. CDiC

A CDiC from our previous work is used as the benchmark [18]. The column in the benchmark CDiC is modeled using the *RadFrac* model with rigorous equilibrium stages. For consistency, the same column model, pressure drop calculations based on Sulzer Mellapak 350Y packing [18], 100% pump efficiency, and the neglect of heat losses and auxiliary loads are applied in the MVR design, ensuring uniformity in the simulation assumptions across both systems.

The column consists of 40 theoretical stages with the feed stage of 33, determined by minimizing the reboiler duty. Two design specifications (Spec/Vary) are set to meet the product purity requirements by adjusting the reflux ratio and distillate flow rate. Following the same baseline settings as in the previous work, the column is operated with the condenser pressure (stage 1) and column overhead pressure (stage 2) both fixed at 1 bar. Under these conditions, the reflux ratio is 1.01, resulting in a condenser duty of 9876 kW and a reboiler duty of 10,073 kW. The slightly lower reboiler duty compared with the previously reported value (10,078 kW) is attributed to the inclusion of a feed pump, which introduces a small additional mechanical energy input.

4.2. MVR

The steady-state simulation results for the four two-stage MVR configurations are presented in this section. To ensure a fair comparison with the D-HIDiC cases reported in our previous work [18], the same compression pressure levels are applied: the first-stage compressor increases the pressure from 1 to 2.5 bar, and the second-stage from 2.5 to 5.029 bar. The compressors are modeled using isentropic compression with a specified isentropic efficiency of 80%. Fig. 2 shows base two-stage MVR configuration without inter-stage cooling (**MVR #1**). The vapor temperature increases from 64.2 °C to 134.5 °C after the first-stage compression and further to 191.7 °C after the second stage, which exceeds typically compressor temperature design limits of 175 °C [26], thus risking compressor damage and safety issue. For practical design, additional compression stages and cooling solutions would therefore be required to maintain safe operation and ensure long-term system reliability. The total compression work is 1850 kW, corresponding to a COP of 5.445. For reference, the D-HIDiC cases **HIDiC #1** and **HIDiC #2** consume 1989 kW and 1936 kW of total compressor power, respectively [18]. Therefore, the MVR outperforms HIDiC for this case study.

To reduce the discharge temperature and recover the sensible heat generated by the first-stage compression, intercooling is introduced in **MVR #2** as shown in Fig. 3. The first-stage discharge stream is cooled from 135.4 to 102 °C by transferring heat to an additional bottom reboiler. At 2.5 bar, the saturated vapor temperature is 89.4 °C, corresponding to a superheat degree of about 12.6 °C; cooling to 102 °C ensures an effective LMTD of 10 °C. With intercooling, the total compression work decreases to 1782 kW and the COP improves to 5.653. In addition, the condenser duty decreases from 1657 kW in **MVR #1** to 1590 kW in **MVR #2**, consistent with the reduction in required compressor power when sensible heat is recovered rather than dissipated.

An intensified alternative to exchanger-based intercooling is liquid injection (**MVR #3**, Fig. 4). Here, approximately 5% of the high-pressure condensate downstream of the main reboiler is injected into the inter-stage vapor stream, cooling it from 135.4 °C to 102 °C, identical to **MVR #2**. In Aspen Plus, the injection rate is determined using the *Design Specs* function in *Flowsheeting Options*, which iteratively adjusts the flow rate until the inter-stage vapor temperature reaches 102 °C. In addition, this direct-contact cooling is modeled using a *Mixer* unit, where the vapor and liquid phases are assumed to undergo ideal mixing and to reach thermodynamic equilibrium at the specified pressure. Pressure drops across the mixing junction are also neglected. Under

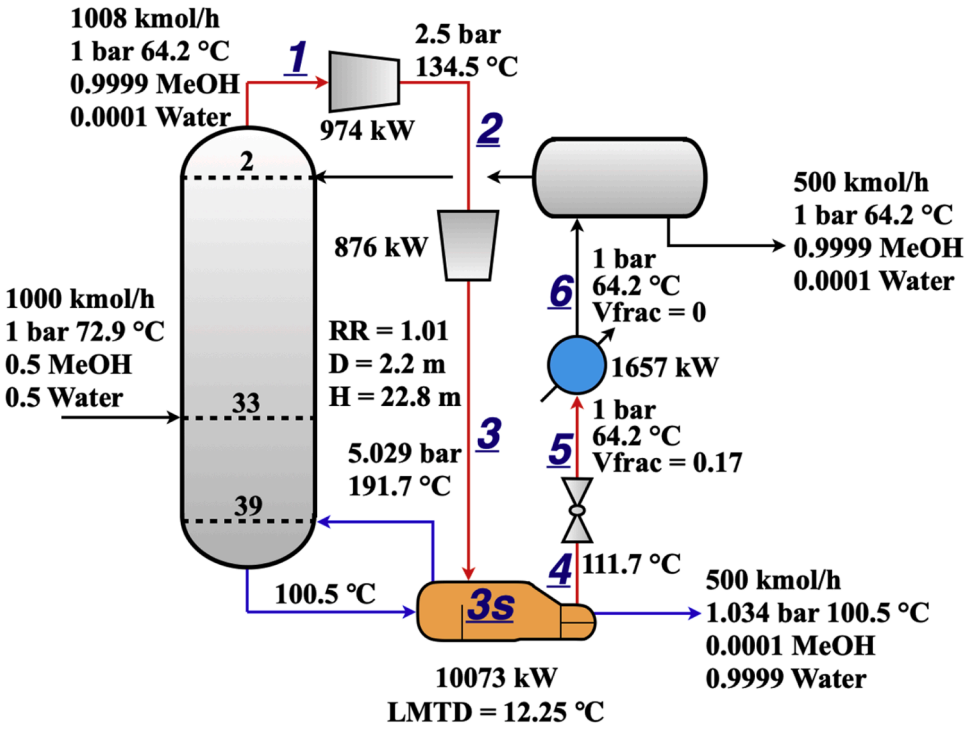

Fig. 2. MVR without intercooling (MVR #1).

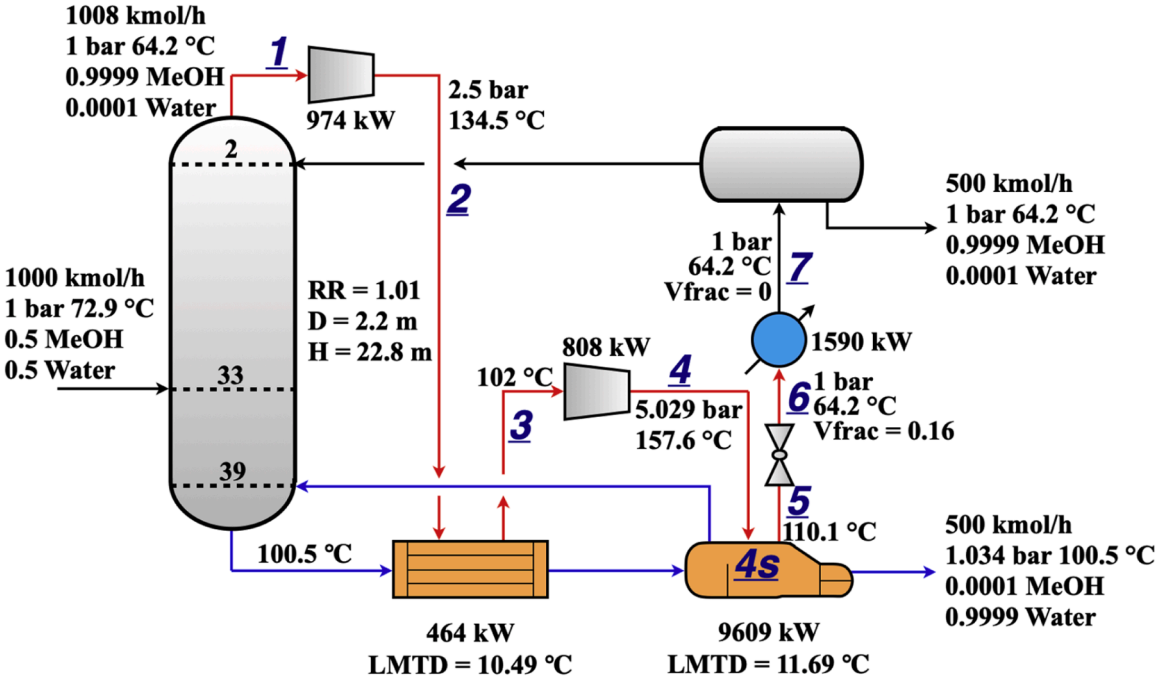

Fig. 3. MVR with intercooling (MVR #2).

these modeling assumptions, the injected liquid absorbs heat from the superheated vapor, thereby reducing the vapor temperature prior to the second-stage compression. Droplet-scale phenomena, such as droplet size distribution, finite evaporation kinetics, and potential maldistribution, are not resolved in the present steady-state flowsheet and are acknowledged as a modeling limitation. In addition, liquid injection increases the total vapor flow rate entering the second-stage compressor. According to Eq. (13), this higher flow rate translates into a higher compressor duty, even through the inlet temperature is reduced. As a result, the second-stage compression work rises from 808 kW to 851 kW, and the total compression work slightly increases to 1825 kW, yielding a COP of 5.519. The condenser duty is 1633 kW, which is 43 kW higher than **MVR #2**. This corresponds directly to the additional compression power required in the second stage ($851 - 808 = 43\ kW$), confirming a consistent energy balance. The performance gap between **MVR #2** and **MVR #3** can potentially be narrowed by implementing pre-compressor splitting.

To mitigate the increased second-stage compression power observed

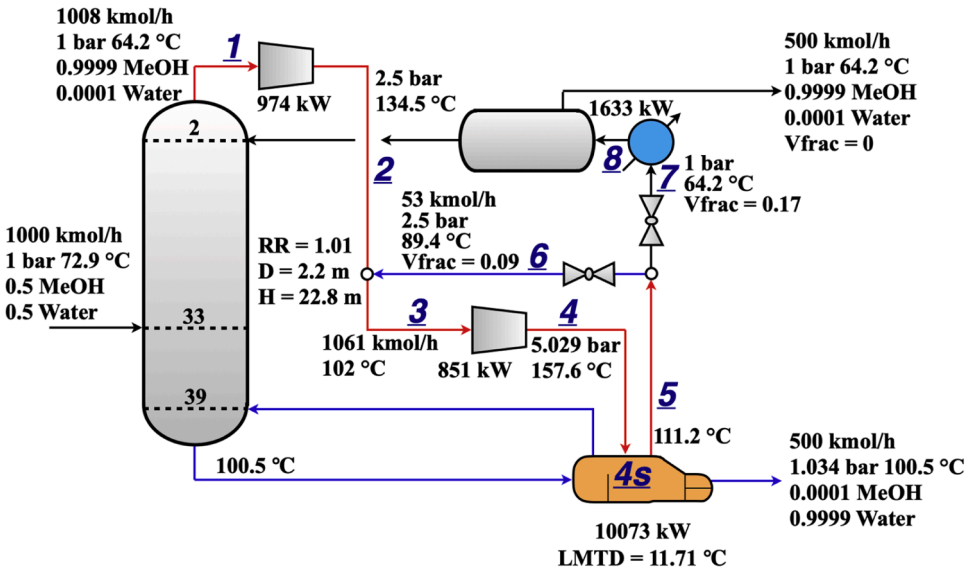

Fig. 4. MVR with liquid injection (MVR #3).

in **MVR #3** while maintaining the compactness benefit of liquid injection, **MVR #4** combines liquid injection with pre-compressor splitting. A fraction of the overhead vapor is bypassed upstream of the first-stage compressor and routed directly to the condenser, thereby reducing the vapor flow through the compression train and improving the distribution of compression duties. The system performance can be tuned by adjusting the split ratio, as shown in Table 1. When the split ratio is 0, **MVR #4** reduces to **MVR #3**. Conversely, increasing the split ratio progressively lowers the total compression work. At a split ratio of 0.0227, **MVR #4** achieves the same total compression work (1782 kW), condenser duty (1590 kW), and COP (5.653) as **MVR #2**, illustrating that pre-compressor splitting can compensate for the additional power introduced by liquid injection. However, the split ratio cannot be increased indefinitely: the maximum feasible value is approximately 0.035 (Fig. 5), beyond which the remaining vapor flow becomes insufficient to provide the required thermal input to the reboiler, leading to an energy deficit. Therefore, an appropriate split ratio must balance reduced compression power against maintaining adequate heat supply for column operation.

4.3. Thermodynamic insights

To further rationalize the thermodynamic behavior of the proposed MVR configurations and to support the discussion on operational feasibility, Fig. 6 summarizes the key state points of **MVR #1 – #4** on both P–h and T–s diagrams, together with the saturated liquid and saturated vapor boundaries of the working mixture (0.9999 methanol/0.0001 water). The diagrams provide a compact validation of the intended sequence of compression, desuperheating, and condensation steps, illustrating how intercooling and liquid injection modify the thermodynamic trajectory at the same overall pressure levels.

Across all configurations, the vapor stream is compressed from the low-pressure to the high-pressure level (1→2→3/4), resulting in an increase in temperature and enthalpy. Subsequent desuperheating and condensation steps shift the high-pressure stream leftward in both diagrams, i.e., toward lower enthalpy and entropy and closer to the saturated liquid curve (blue), consistent with heat rejection to the reboiler. The saturated vapor curve (red) is particularly useful for interpreting compressor operability, since trajectories moving into the two-phase region would imply the presence of liquid during compression.

For **MVR #1**, desuperheating/condensation primarily occurs in the reboiler, followed by further condensation in the condenser. For **MVR #2**, the addition of an inter-stage cooler reduces the inlet temperature to the second compression stage, which is reflected by a lower inter-stage temperature level on the T–s plot (2→3) and a moderated discharge condition at the high-pressure level; this is consistent with a reduction in compression duty relative to a fully uncooled two-stage path.

For the liquid injection configurations (**MVR #3** and **MVR #4**), the additional injection/mixing step appears as an approximately constant-pressure lateral shift on both diagrams (highlighted in purple), representing enthalpy and temperature moderation of the compressed vapor by mixing with a colder stream. Because the injection stream is expanded through a valve upstream of the mixer, partial flashing occurs and the stream enters the mixer as a two-phase vapor-liquid mixture, but the key point from Fig. 6 is that the second-stage compressor suction states remain on the vapor side of the saturation boundary. This provides a qualitative thermodynamic check confirming that liquid injection can serve as a temperature-control mechanism, while practical implementation requires appropriate injection and vapor-liquid disengagement arrangements (e.g., nozzles, separators, coalescers) to avoid liquid

Table 1
The effect of pre-compressor split ratio on MVR performances.

Pre-compressor split ratio β	Compressor 1 duty (kW)	Compressor 2 duty (kW)	Total compression duty (kW)	Condenser duty (kW)	COP
0	974	851	1825	1633	5.519
0.005	969	846	1815	1623	5.550
0.01	965	842	1807	1614	5.574
0.015	960	837	1797	1604	5.605
0.02	955	833	1788	1595	5.634
0.0227	952	830	1782	1590	5.653
0.025	950	828	1778	1586	5.665
0.03	945	824	1769	1576	5.694
0.035	940	819	1759	1567	5.727

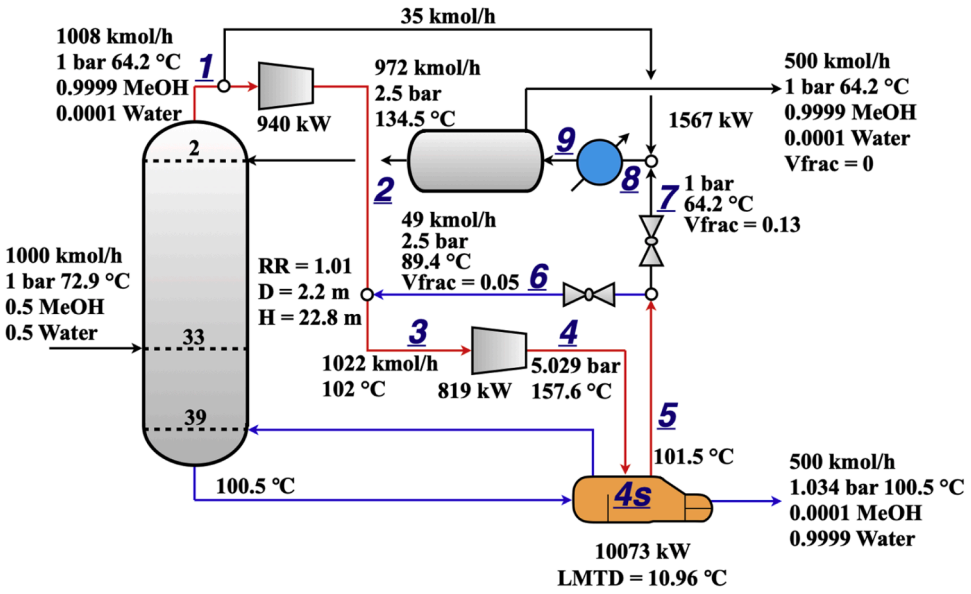

Fig. 5. MVR with liquid injection and pre-compressor splitting (MVR #4).

carryover to the compressor.

Finally, for **MVR #4**, the reboiler outlet is predicted to be slightly subcooled after condensation. The subsequent enthalpy increase caused by mixing with the pre-compressor split stream (states 1 and 7 forming state 8) is then removed in the condenser.

4.4. Energy performance evaluation

The energy performance of the studied configurations is assessed from two complementary perspectives: energy quantity and energy quality. Here, energy quantity refers to the final energy input required by the process (external heat for CDiC versus electricity for MVR). Energy quality is evaluated through an equivalent primary energy comparison, which accounts for the upstream conversion needed to generate electricity.

For the benchmark CDiC, ideal boiler efficiency (100%) is assumed for the conversion of primary energy to steam utility (in reality, the boiler efficiencies typically range from 85% to 90%). Under the specified product purities, CDiC requires 10,073 kW of reboiler duty. For the MVR-based processes, the final energy input is the compressor power. As summarized in Table 2, MVR can save approximately 80% final energy input relative to CDiC, demonstrating the strong potential of electrified vapor recompression for reducing direct process energy demand. Among the studied cases, **MVR #4** achieves the lowest compressor power, followed by **MVR #2**. MVR configurations outperform HIDiC in terms of compressor duty and primary energy savings. However, these results are specific to the methanol/water system and the operational conditions studied. In other systems, the advantages of MVR might not be as pronounced, and HIDiC could still offer competitive performance.

Because electricity is a higher-grade energy form than low-temperature process heat, a primary energy perspective is also considered. Following the assumption adopted in this work, compressor electricity is converted to an equivalent primary fuel energy using a power generation efficiency of 36.6% [27]. For the benchmark CDiC, the primary energy is conservatively taken as equal to the reboiler duty (i.e., assuming ideal conversion from primary fuel to process heat; accounting for real boiler efficiency would increase the primary-energy requirement of CDiC, further strengthening the relative advantage of the MVR cases).

With this conversion, the MVR configurations achieve approximately 50% primary energy savings compared with CDiC. The best primary-energy performance is obtained by **MVR #4** (52.29%), closely followed by **MVR #2** (51.66%). The results indicate that intercooling heat recovery improves the power requirement (**MVR #2**), while liquid injection can deliver a more compact intensified configuration with competitive energy performance when combined with pre-compressor splitting (**MVR #4**).

It should be noted that the incremental efficiency gain of **MVR #4** over the well-designed intercooled case **MVR #2** is modest for this case study (0.23% in energy-quantity savings and 0.63% in primary-energy savings), indicating that the main advantage of liquid injection is not a large standalone efficiency increase.

4.5. Indicative economic implications

To complement the energy evaluation in Section 4.4, an indicative economic screening is performed based on the cost correlations and assumptions summarized in Table 3, with a CAPEX/OPEX/TAC comparison reported in Table 4.

As shown in Table 4, moving from the benchmark CDiC to the MVR configurations increases total CAPEX from 1.1 M USD to approximately 6.5 M USD, as the compressor packages become the dominant capital contributors. Nevertheless, the compactness benefit associated with liquid injection is reflected at equipment level: the inter-stage cooler required in **MVR #2** (0.2 M USD) is eliminated in **MVR #3** and **MVR #4**, simplifying the two-stage compression train and reducing heat exchanger hardware. This equipment simplification can be a significant benefit in space-constrained revamps or brownfield installations, even when the efficiency difference relative to exchanger-based intercooling is small. Within the MVR family, the highest CAPEX is observed for **MVR #2** (6.58 M USD) due to the added inter-stage cooler and comparatively higher compressor-related costs, whereas the lowest CAPEX is achieved by **MVR #4** (6.39 M USD), which combines liquid injection with pre-compressor splitting and shows reduced compressor costs. In terms of OPEX, all MVR options substantially reduce energy cost relative to CDiC: OPEX decreases from 2.26 M USD/yr (CDiC) to 0.85–0.90 M USD/yr (MVR), corresponding to approximately 60% OPEX savings. When CAPEX and OPEX are considered together through TAC, the MVR configurations remain economically attractive under the assumed economics, with TAC reduced from 2.37 M USD/yr (CDiC) to 1.49–1.55 M USD/yr (MVR), approximately 35% TAC savings.

Among the evaluated designs, **MVR #4** delivers the best overall economics, achieving the lowest OPEX and the lowest TAC, which is consistent with its dual benefit of (i) eliminating the inter-stage cooler and (ii) reducing total compression duty via pre-compressor splitting. By

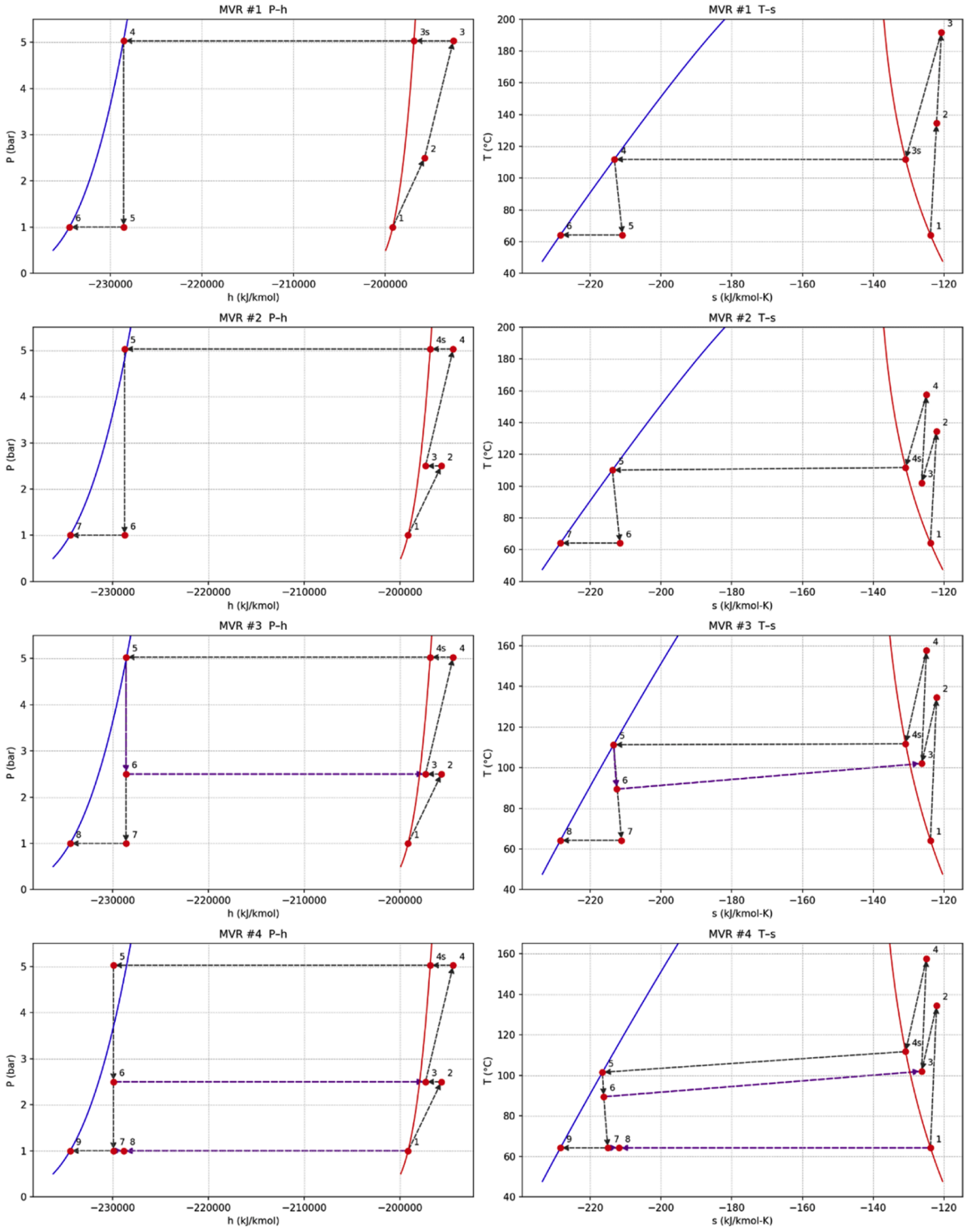

Fig. 6. P–h diagram and T–s diagram for different configurations.

Table 2
Energy consumption comparison for different configurations.

	CDiC	HIDiC #1 [18]	HIDiC #2 [18]	MVR #1	MVR #2	MVR #3	MVR #4
COP	-	5.067	5.206	5.445	5.653	5.519	5.727
Energy quantity (kW)	10,073	1989	1936	1850	1782	1825	1759
Energy quantity saving	0	80.25%	80.78%	81.63%	82.31%	81.88%	82.54%
Primary energy savings	0	46.05%	47.49%	49.82%	51.66%	50.50%	52.29%

contrast, **MVR #3** eliminates the intercooler but retains a slightly higher OPEX and TAC, indicating that liquid injection alone improves

Table 3
Basis of Economics [28].

Distillation column vessel (diameter and length in meters)
$CAPEX = 17,640(D)^{1.066}(L)^{0.802}$
Condenser (area in m^2)
Heat transfer coefficient $= 0.852\ kW/(^{\circ}C{\cdot}m^2)$
Differential temperature $=$ *Reflux drum temperature* $- 30\ ^{\circ}C$
$CAPEX = 7,296(A)^{0.65}$
Reboiler (area in m^2)
Heat transfer coefficient $= 0.568\ kW/(^{\circ}C{\cdot}m^2)$
$CAPEX = 7,296(A)^{0.65}$
Inter-stage cooler (area in m^2)
Heat transfer coefficient $= 0.28\ kW/(^{\circ}C{\cdot}m^2)$
$CAPEX = 7,296(A)^{0.65}$
Compressor (work in horsepower)
$CAPEX = (1,293)(517.3)(3.11)(hp)^{0.82}/280$
OPEX
Low-pressure steam (6 bar, 160 °C) $= 7.78$ USD/GJ
Electricity $= 16.8$ USD/GJ
Total annual cost (USD/yr)
$TAC = \frac{CAPEX}{Payback\ period} + OPEX$
Payback period $= 10$ yr

Table 4
TAC comparison for different configurations.

Cost	CDiC	MVR #1	MVR #2	MVR #3	MVR #4
CAPEX (USD)					
Column	501,863	501,863	501,863	501,863	501,863
Condenser	321,842	100,871	98,183	99,892	97,266
Reboiler	294,456	827,146	826,769	851,705	888,936
Inter-stage cooler	-	-	196,019	-	-
Compressor 1	-	2667,878	2667,878	2667,836	2591,048
Compressor 2	-	2444,040	2288,539	2387,497	2314,923
Total CAPEX	1118,161	6541,798	6579,250	6508,794	6394,035
OPEX (USD/yr)	2257,056	895,039	862,402	883,108	851,403
OPEX saving	0	60.34%	61.79%	60.87%	62.28%
TAC (USD/yr)	2368,872	1549,219	1520,327	1533,988	1490,807
TAC saving	0	34.60%	35.82%	35.24%	37.07%

compactness but may not fully minimize compression work unless coupled with an appropriate vapor split strategy.

Overall, this indicative assessment supports that liquid-injection-based intensification can remain economically competitive, and that pre-compressor splitting is a practical lever to simultaneously improve compactness and reduce operating cost. Finally, the values in Table 4 are intended for comparative screening; utility price ratios, compressor package scope, and project-specific installation factors may shift absolute costs, and a detailed design-stage economic study (e.g., with vendor quotations) would be required for investment decisions.

4.6. Comments on dynamics and control

Liquid injection and pre-compressor splitting introduce additional degrees of freedom in multi-stage MVR systems. While the present study focuses on steady-state design screening and energy comparisons, dynamic response and controllability are important considerations for industrial implementation. Prior work has reported relevant insights for related MVR with pre-compressor splitting. Luyben [29] showed that the pre-compressor splitting can be well-regulated by controlling the downstream pressure using a control valve. In addition, the dynamic behavior of liquid injection has been examined in our earlier study on D-HIDiC, where robust dynamic performance was demonstrated without adverse dynamic interactions [19]. These literature findings support the feasibility of using liquid injection and/or pre-compressor splitting as a responsive handle for temperature management. A rigorous dynamic assessment of the four MVR configurations is beyond the scope of the current paper.

4.7. Practical implications and implementation challenges

The results provide several practical implications for industrial electrified distillation. First, multi-stage MVR offers an electrification route for wide-boiling separations where single-stage vapor recompression becomes impractical due to excessive pressure ratios. For the studied case, the multi-stage MVR schemes reduce the final energy input by about 80% relative to conventional distillation and deliver around 50% primary-energy savings under a fossil-based electricity assumption. Second, replacing exchanger-based intercooling with liquid injection simplifies the compression train by eliminating an intercooler and associated piping, which is attractive for revamps and brownfield applications where plot space and equipment count are critical. Third, pre-compressor splitting provides an effective tuning degree of freedom to offset the additional second-stage load introduced by liquid injection and to recover energy performance comparable to an intercooled design while retaining the compactness benefit.

Several challenges remain before implementation. Liquid injection system requires detailed mechanical design to ensure stable and uniform distribution and effective vapor-liquid disengagement, such that no liquid carryover reaches the compressor stages. Long-term compressor reliability under potential intermittent “wet” conditions should be verified against vendor specifications, including appropriate safeguards and separation provisions. In addition, although the present work focuses on steady-state screening, dynamic assessment and control-structure synthesis are needed to quantify disturbance rejection and to define practical operating policies when liquid injection and/or pre-compressor split ratio are used as additional operating handles. Finally, extending the concept beyond the methanol/water case to strongly non-ideal and multicomponent mixtures will require further validation, since fluid properties and phase behavior may alter feasible operating windows and equipment constraints.

4.8. Comments on decarbonization potential

The primary energy analysis in this study uses a fossil-based power plant efficiency of 36.6% as a baseline. While this is appropriate for conventional power generation, it does not fully capture the potential of renewable electricity and energy storage systems in future grid mixes. As renewable energy sources, such as solar and wind, paired with battery storage or grid balancing technologies, become more prevalent, the

effective efficiency of electricity generation can increase significantly. For example, renewable electricity generation could achieve effective efficiencies approaching 80 – 90% [30] when considering the full life-cycle of renewables and energy storage, compared with fossil-based systems.

In this context, the primary-energy savings of around 50% for MVR vs. CDiC are conservative estimates. They reflect the energy savings achievable with a fossil-based power grid but may understate the decarbonization potential when cleaner power mixes are used. A shift to renewable electricity would not only enhance the energy savings but also further reduce the carbon footprint of the system, potentially bringing MVR systems much closer to net-zero emissions and supporting broader decarbonization goals in industrial sectors. This highlights the importance of considering the grid energy mix when assessing the decarbonization of MVR-based electrified distillation.

5. Scope and limitations

This study evaluates multi-stage MVR configurations for a single binary system (methanol/water) at a specific feed condition (1000 kmol/h, saturated liquid feed at 1 bar) and high product purities (99.99 mol% for both products). Under identical column specifications and modeling assumptions, the comparative trends among CDiC, D-HIDiC, and the proposed MVR options remain consistent, and the incremental effects of intercooling, liquid injection, and pre-compressor splitting can be traced to the mechanisms summarized in Section 3.2. Nevertheless, this does not imply universal applicability across all separations; the quantitative benefits will depend on mixture properties and separation difficulty.

Methanol/water is a non-ideal binary mixture, and it is modeled using NRTL in this work. At the same time, it is zeotropic over the investigated conditions and exhibits smooth phase behavior, which makes it a well-suited test case to isolate the role of temperature lift and compression superheating in multi-stage MVR. The large boiling-point difference results in a substantial overall temperature lift, and the bell-shaped P–h saturation envelope means that compression readily produces significant superheating. This can be linked directly to the compressor temperature relation: according to Eq. (6), the discharge temperature increases with the pressure ratio Π and depends on the heat capacity ratio γ, so large pressure ratios amplify superheating and make inter-stage conditioning particularly influential on discharge temperature and compression duty.

The most relevant fluid-property effects for MVR thermodynamic performance are those entering the governing energy relationships: the caloric behavior of the vapor phase (captured via γ in Eq. (6)) and the enthalpy surface of the mixture (including the enthalpy of vaporization and the P–h saturation envelope), which together determine the attainable temperature levels and the amount of upgraded heat per unit mass of recompressed vapor. Mixture non-ideality primarily manifests through phase equilibrium (activity coefficients), shaping the column temperature/composition profiles and thus the temperature levels at which reboiling and condensation occur. In contrast, transport properties such as viscosity (and, more generally, heat-transfer and hydraulic characteristics) primarily affect equipment-level design (heat-transfer coefficients, pressure drops, and exchanger/column sizing) rather than the thermodynamic trends of compressor duty and COP central to the steady-state comparisons.

Several limitations should be noted. First, only one binary system and one set of feed/product specifications are examined; different throughput, feed state, pressure levels, or purity targets could change optimal staging and the relative importance of sensible-heat recovery. Second, for other mixtures—especially those with markedly different γ, latent heats, and saturation-envelope shapes over the relevant pressure range—the degree of compression superheating (Eq. (6)) and the effectiveness of intercooling/injection may differ, which can shift the relative ranking of configurations. Third, the presence of an azeotrope does not by itself preclude MVR, but it often implies different separation configurations (e.g., pressure-swing or extractive distillation) and more complex temperature/duty profiles; the main implication for MVR integration is then the thermal matching between the recompressed-vapor temperature level and the column heat-demand profile, rather than the mere existence of an azeotrope.

Finally, the liquid injection and mixing steps are represented using steady-state, equilibrium-based unit operations; droplet-scale effects (finite evaporation, maldistribution, disengagement, and potential liquid carryover) are not resolved and must be addressed in detailed mechanical design and dynamic studies. Overall, the present work provides a transparent steady-state screening and thermodynamic interpretation for a representative wide-boiling, non-azeotropic system. Future work should extend the assessment to additional mixtures and separation classes and incorporate systematic optimization of staging and injection/split variables under practical equipment constraints and vendor limits.

6. Conclusions

This study investigated process intensification of multi-stage heat-pump-assisted distillation by introducing liquid injection as an alternative to exchanger-based intercooling in a two-stage MVR system. Four MVR configurations were designed and evaluated under identical column specifications and compression pressure levels, and benchmarked against a CDiC and reported D-HIDiC cases.

Overall, the results confirm that electrified vapor recompression can markedly reduce the external energy input for this wide-boiling methanol/water separation. Across the studied designs, the MVR schemes reduce the final energy input by approximately 80% relative to CDiC, and this advantage remains when assessed on a primary-energy basis. Introducing intercooling with heat recovery (**MVR #2**) decreases the overall compression demand by lowering the second-stage inlet temperature and reintegrating the sensible heat generated during the first-stage compression.

Liquid injection (**MVR #3**) provides a compact intensification option by eliminating an intercooling heat exchanger, while still achieving comparable thermodynamic trajectories in the P–h and T–s representations. However, liquid injection increases the second-stage load due to the increased vapor flow entering the second-stage compressor. Combining liquid injection with pre-compressor splitting (**MVR #4**) effectively mitigates this drawback and provides a practical tuning degree of freedom to redistribute compressor loading and recover efficiency without adding hardware complexity. For the studied methanol/water case, the efficiency improvement over exchanger-based intercooling is incremental; the primary added value of the injection-based schemes lies in hardware simplification and the additional tunability enabled by the split ratio.

Finally, while the present work provides a transparent steady-state screening and thermodynamic interpretation, further work is needed to extend the assessment to other mixtures (especially strongly non-ideal or azeotropic systems), and to address equipment-level implementation aspects such as injection hardware design, vapor-liquid disengagement, and dynamic behavior under disturbances.

CRediT authorship contribution statement

Chengtian Cui: Writing – original draft, Validation, Supervision, Software, Resources, Investigation, Formal analysis, Conceptualization. **Anton A. Kiss:** Validation, Supervision, Methodology, Investigation, Funding acquisition, Formal analysis, Conceptualization.

Declaration of competing interest

The authors declare that they have no known competing financial interests or personal relationships that could have appeared to influence

the work reported in this paper.

Acknowledgments

This work was supported by the Marie Skłodowska-Curie Actions Postdoctoral Fellowship (Grant No. 101211557).

Data availability

Data will be made available on request.

References

[1] T.J. Mathew, S. Narayanan, A. Jalan, L. Matthews, H. Gupta, R. Billimoria, C. S. Pereira, C. Goheen, M. Tawarmalani, R. Agrawal, Advances in distillation: significant reductions in energy consumption and carbon dioxide emissions for crude oil separation, Joule 6 (2022) 2500–2512, https://doi.org/10.1016/j.joule.2022.10.004.
[2] A.A. Kiss, R. Smith, Rethinking energy use in distillation processes for a more sustainable chemical industry, Energy 203 (2020) 117788, https://doi.org/10.1016/j.energy.2020.117788.
[3] C. Cui, M. Qi, X. Zhang, J. Sun, Q. Li, A.A. Kiss, D.S.-H. Wong, C.M. Masuku, M. Lee, Electrification of distillation for decarbonization: an overview and perspective, Renew. Sustain. Energy Rev. 199 (2024) 114522, https://doi.org/10.1016/j.rser.2024.114522.
[4] Z. Mekidiche, J.A. Labarta, J. Javaloyes-Anton, J.A. Caballero, From power to heat: strategies for electrifying distillation for sustainable chemical processes, Appl. Therm. Eng. 257 (2024) 124316, https://doi.org/10.1016/j.applthermaleng.2024.124316.
[5] M. Adami, K. Farheen, M. Skiborowski, Electrifying distillation – optimization-based evaluation of internally heat-integrated distillation columns, Sep. Purif. Technol. 360 (2025) 131061, https://doi.org/10.1016/j.seppur.2024.131061.
[6] M. Adami, J. Schnurr, M. Skiborowski, Electrified distillation – Optimized design of closed cycle heat pumps with refrigerant selection and flash-enhanced mechanical vapor recompression, Appl. Therm. Eng. 273 (2025) 126559, https://doi.org/10.1016/j.applthermaleng.2025.126559.
[7] M. Qi, X. Zhang, D.S. Wong, C. Shu, C. Cui, A.A. Kiss, Electrified distillation with flash vapor circulation and thermal storage for dynamic electricity markets, AIChE J. (2025), https://doi.org/10.1002/aic.18750.
[8] C. Cui, N.V.D. Long, J. Sun, M. Lee, Electrical-driven self-heat recuperative pressure-swing azeotropic distillation to minimize process cost and CO<inf>2</inf>emission: process electrification and simultaneous optimization, Energy 195 (2020), https://doi.org/10.1016/j.energy.2020.116998.
[9] A.A. Kiss, C.A. Infante Ferreira, Heat Pumps in Chemical Process Industry, CRC Press, 2016, https://doi.org/10.1201/9781315371030.
[10] A.A. Kiss, S.J. Flores Landaeta, C.A. Infante Ferreira, Towards energy efficient distillation technologies – Making the right choice, Energy 47 (2012) 531–542, https://doi.org/10.1016/j.energy.2012.09.038.
[11] W.L. Luyben, Capital cost of compressors for conceptual design, Chem. Eng. Process. - Process Intensif. 126 (2018) 206–209, https://doi.org/10.1016/j.cep.2018.01.020.
[12] H. Luo, C.S. Bildea, A.A. Kiss, Novel heat-pump-assisted extractive distillation for bioethanol purification, Ind. Eng. Chem. Res. 54 (2015) 2208–2213, https://doi.org/10.1021/ie504459c.
[13] H. Shahandeh, M. Jafari, N. Kasiri, J. Ivakpour, Economic optimization of heat pump-assisted distillation columns in methanol-water separation, Energy 80 (2015) 496–508, https://doi.org/10.1016/j.energy.2014.12.006.
[14] A.A. Shenvi, D.M. Herron, R. Agrawal, Energy efficiency limitations of the conventional heat integrated distillation column (HIDiC) configuration for binary distillation, Ind. Eng. Chem. Res. 50 (2011) 119–130, https://doi.org/10.1021/ie101698f.
[15] M. Aurangzeb, A.K. Jana, Vapor recompression with interreboiler in a ternary dividing wall column: improving energy efficiency and savings, and economic performance, Appl. Therm. Eng. 147 (2019) 1009–1023, https://doi.org/10.1016/j.applthermaleng.2018.11.008.
[16] W.L. Luyben, Control of a recuperative vapor- recompression air separation process, J. Process Control 45 (2016) 55–64, https://doi.org/10.1016/j.jprocont.2016.06.007.
[17] C. Cui, X. Zhang, M. Qi, H. Lyu, J. Sun, A.A. Kiss, Fully electrified heat pump assisted distillation process by flash vapour circulation, Chem. Eng. Res. Des. 206 (2024) 280–284, https://doi.org/10.1016/j.cherd.2024.05.011.
[18] C. Cui, J. van Reisen, I. Tyraskis, A.A. Kiss, Efficient heat integration within discretely heat integrated distillation columns using liquid injection, AIChE J. (2025), https://doi.org/10.1002/aic.18861.
[19] C. Cui, Q. Li, W.L. Luyben, A.A. Kiss, Dynamics and control of discretely heat integrated distillation columns, Comput. Chem. Eng. (2025) 109144, https://doi.org/10.1016/j.compchemeng.2025.109144.
[20] C.W. Roh, M.S. Kim, Effects of intermediate pressure on the heating performance of a heat pump system using R410A vapor-injection technique, Int. J. Refrig. 34 (2011) 1911–1921, https://doi.org/10.1016/j.ijrefrig.2011.07.011.
[21] H. Zou, X. Li, M. Tang, J. Wu, C. Tian, D. Butrymowicz, Y. Ma, J. Wang, Temperature stage matching and experimental investigation of high-temperature cascade heat pump with vapor injection, Energy 212 (2020) 118734, https://doi.org/10.1016/j.energy.2020.118734.
[22] E. Torrella, J.A. Larumbe, R. Cabello, R. Llopis, D. Sanchez, A general methodology for energy comparison of intermediate configurations in two-stage vapour compression refrigeration systems, Energy 36 (2011) 4119–4124, https://doi.org/10.1016/j.energy.2011.04.034.
[23] X. Jin, J. Zhang, Z. Liu, W. Hong, S. Sha, Z. Qiu, Z. Wu, W. Su, Performance analysis of a two-stage vapor compression heat pump based on intercooling effect, Case Stud. Therm. Eng. 51 (2023) 103643, https://doi.org/10.1016/j.csite.2023.103643.
[24] L. Zhang, Y. Jiang, J. Dong, Y. Yao, Advances in vapor compression air source heat pump system in cold regions: a review, Renew. Sustain. Energy Rev. 81 (2018) 353–365, https://doi.org/10.1016/j.rser.2017.08.009.
[25] A. Rix, N. Paul, L. Wessner, D. Murrenhoff, Optimization of heat pump and vapor recompression technologies for wide-boiling mixtures, in: F. Manenti, G. V. Reklaitis (Eds.), Book of Abstract of the 34th European Symposium on Computer Aided Process Engineering /15th International Symposium on Process Systems Engineering (ESCAPE34/PSE24), Florence, Italy, 2024, pp. 275–280.
[26] W.L. Luyben, Compressor heuristics for conceptual process design, Ind. Eng. Chem. Res. 50 (2011) 13984–13989, https://doi.org/10.1021/ie202027h.
[27] K. Matsuda, Y. Kansha, C. Fushimi, A. Tsutsumi, A. Kishimoto, Advanced Energy Saving and Its Applications in Industry, Springer London, London, 2013, https://doi.org/10.1007/978-1-4471-4207-2.
[28] W.L. Luyben, Principles and Case Studies of Simultaneous Design, Wiley, 2011, https://doi.org/10.1002/9781118001653.
[29] W.L. Luyben, Control of an azeotropic DWC with vapor recompression, Chem. Eng. Process. - Process Intensif. 109 (2016) 114–124, https://doi.org/10.1016/j.cep.2016.08.013.
[30] O. Ellabban, H. Abu-Rub, F. Blaabjerg, Renewable energy resources: current status, future prospects and their enabling technology, Renew. Sustain. Energy Rev. 39 (2014) 748–764, https://doi.org/10.1016/j.rser.2014.07.113.